Hall-magnetohydrodynamic turbulence

V Krishan[1] and S M Mahajan[2]

1: *Indian Institute of Astrophysics, Bangalore 560 034, India; e-mail:vinod@iiap.res.in*

2: *Institute for Fusion Studies, The University of Texas at Austin, Austin, Texas 78712, USA*

1. Introduction

Turbulence is as ubiquitous in nature as it is elusive. The fact, that it is not mere randomness, merits more exploration. Coherent structures, correlated motions and well- defined patterns are observed on a variety of spatial and temporal scales in otherwise turbulent media. Organized states of matter and motion can be seen in, convection cells, cloud complexes, tornados, cyclones, zonal flows on planetary surfaces, the Red Spot of Jupiter, solar and stellar granulation, spiral patterns of galaxies and perhaps ourselves! The universality of its(turbulence) existence has inspired the investigators to look for universal characteristics such as the large Reynolds Number, a consequence of the large nonlinearity. The dimensional arguments of a la Kolmogoroff to delineate the spectral distributions has proved to be another rewarding route to pursue this otherwise forbidding field. The Taylor Relaxation hypothesis is a further attempt to understand the evolution of any nonlinear system in terms of its global properties such as the invariants. The macroscopic turbulence is often modeled using ideal magnetohydrodynamics. We determine the spectra of the velocity and the magnetic field fluctuations within the framework of the two fluid picture including specifically the Hall effect. It is shown that the Hall magnetohydrodynamics (HMHD) supports three quadratic invariants viz the total energy, the magnetic helicity and the generalized helicity. The nonlinear states depart fundamentally from the Alfvénic state challenging the much believed concept of the equipartition of the kinetic and the magnetic energy densities. Using the dimensional arguments "a la Kolmogoroff", we derive the spectral energy distributions corresponding to the three invariants. These distributions are stringed together by invoking the hypothesis of the selective dissipation which has proved its efficacy in the two- dimensional hydrodynamic turbulence. We apply the results to three different situations namely: (i) the solar wind spectra, (ii) the solar atmospheric turbulence, the solar granulation, and (iii) the laboratory experiments.

The model reproduces in the inertial range the three branches of the observed solar wind magnetic fluctuation spectrum - the Kolmogorov branch $f^{-5/3}$ steepening to $f^{-\alpha_1}$ with $\alpha_1 \simeq$ 3-4 on the high frequency side and flattening to f^{-1} on the low frequency side. These fluctuations are found to be associated with the nonlinear Hall-MHD Shear Alfvén waves. The spectrum of the concomitant whistler type fluctuations is very different from the observed one. Perhaps the relatively stronger damping of the whistler fluctuations may cause their unobservability.

The additional structure imparted to the spectral laws (by the inclusion of the generalized helicity) allows us to reproduce, remarkably well, the essentials as well as the details of the observed spectra of the motions and the magnetic fields of the solar atmosphere on the scales of a few thousand kilometers.

In a recent study, the properties of the large scale turbulence have been investigated theoretically and experimentally concluding that the kinetic energy spectrum goes as $k^{1/3}$ at large spatial scales and citing a few examples for the existence of such a spectrum in natural systems. We showed that the 1/3 spectrum for the kinetic energy is a direct consequence of the magnetic helicity invariant of the Hall- MHD turbulence. We present the simultaneous kinetic and magnetic energy spectra and propose the verification of the latter in the laboratory and natural systems. The paper ends with some possible future directions of research in this field. The essentials of the Hall- Magnetohy-

drodynamics (HMHD)have been presented in section 2. The key aspects along with a discussion of the quadratic invariants, are summarized in Section 3. In Section 4, the respective spectral energy distributions are derived. The spectral distributions so obtained are then compared and contrasted with the inferred distributions on the solar wind (section 5), solar granulation (section 6) and the laboratory experiments (section 7). Naturally the new element, the generalized helicity, and its consequences will spell the departure of this work from the previous literature.

2. Hall-MHD system

In the HALL-MHD, comprising of the two fluid Model, the electron fluid equation is given by

$$m_e n_e \left[\frac{\partial \boldsymbol{V}_e}{\partial t} + (\boldsymbol{V}_e.\nabla)\boldsymbol{V}_e\right] = -\nabla p_e - e n_e \left[\boldsymbol{E} + \frac{1}{c}\boldsymbol{V}_e \times \boldsymbol{B}\right] \tag{1}$$

Assuming inertialess electrons ($m_e \to 0$), the electric field is found to be:

$$\boldsymbol{E} = -\frac{1}{c}\boldsymbol{V}_e \times \boldsymbol{B} - \frac{1}{n_e e}\nabla p_e. \tag{2}$$

The Ion fluid equation is :

$$m_i n_i \left[\frac{\partial \boldsymbol{V}_i}{\partial t} + (\boldsymbol{V}_i.\nabla)\boldsymbol{V}_i\right] = -\nabla p_i + e n_i \left[\boldsymbol{E} + \frac{1}{c}\boldsymbol{V}_i \times \boldsymbol{B}\right] \tag{3}$$

Substitution for $\boldsymbol{E}$ from the inertialess electron Eq. begets:

$$m_i n_i \left[\frac{\partial \boldsymbol{V}_i}{\partial t} + (\boldsymbol{V}_i.\nabla)\boldsymbol{V}_i\right] = -\nabla(p_i + p_e) + \frac{1}{c}\boldsymbol{J} \times \boldsymbol{B}. \tag{4}$$

The magnetic Induction Eq. becomes:

$$\frac{\partial \boldsymbol{B}}{\partial t} = -c\nabla \times \boldsymbol{E} = \nabla \times (\boldsymbol{V}_e \times \boldsymbol{B}), \tag{5}$$

where $\boldsymbol{B}$ is seen to be frozen to electrons.

Substituting for $\boldsymbol{V}_e = \boldsymbol{V}_i - \boldsymbol{J}/en$, one gets :

$$\frac{\partial \boldsymbol{B}}{\partial t} = \nabla \times \left(\boldsymbol{V}_i - \frac{\boldsymbol{J}}{en}\right) \times \boldsymbol{B}. \tag{6}$$

We see that $\boldsymbol{B}$ is not frozen to the ions, $n_e = n_i = n$.

The Hall term dominates for $(nec)^{-1}\boldsymbol{J} \times \boldsymbol{B} \geq \boldsymbol{V}_i \times \boldsymbol{B}/c$ or $L \leq M_A c/\omega_{pi}$ and $T \geq \omega_{ci}^{-1}$, where L is the length scale, ω_{pi} is the ion plasma frequency and ω_{ci} is the ion cyclotron frequency. The Hall term decouples electron and ion motion on ion inertial length scales and ion cyclotron times. Hall effect does not affect mass and momentum transport but it does affect the energy and magnetic field transport.

3. HMHD, nonlinear solution, invariants

It is well known that the Alfvénic state is an exact solution of the nonlinear MHD [1]. This prompts one to speculate if a similar kind of an exact solution exists for Hall MHD (HMHD), a system which encompasses MHD, but can sustain a much richer spectrum of plasma states not accessible to MHD.

In the Alfvénic units with the magnetic field $\boldsymbol{B}$ normalized to an ambient field, the velocity $\boldsymbol{V}$ normalized to the corresponding Alfvén speed, time and space variables, respectively, measured in units of the ion gyroperiod $\omega_c^{-1} = mc/qB_0$, and the ion skin depth $\lambda_i = c/\omega_{pi}$, where $\omega_{pi} = (4\pi q^2 n/m_i)^{1/2}$ is the ion plasma frequency. the following dimensionless equations

$$\frac{\partial \boldsymbol{B}}{\partial t} = \nabla \times [(\boldsymbol{V}_i - \nabla \times \boldsymbol{B}) \times \boldsymbol{B}], \tag{7}$$

$$\frac{\partial (\boldsymbol{B} + \nabla \times \boldsymbol{V}_i)}{\partial t} = \nabla \times [\boldsymbol{V}_i \times (\boldsymbol{B} + \nabla \times \boldsymbol{V}_i)], \tag{8}$$

constitute Hall MHD.

Notice that in Eq. (8), obtained by taking the curl of the ion force balance equation, the pressure gradient term $\nabla p/n$ has disappeared because it has been assumed to be a perfect gradient (by invoking an equation of state $p = p(n)$, for example); the pressure has not been neglected.

We will, first, recount the essential elements of the recently found fully nonlinear wave sustained by Hall MHD [2]. This arbitrary amplitude wave contains the standard Alfvénic (Whistler) nonlinear state as its long (short) wavelength limit. The most important aspect of this wave is the wave-number dependent relationship

$$\boldsymbol{B}_k = \alpha(k)\boldsymbol{V}_k, \tag{9}$$

between the fluctuating magnetic field $\boldsymbol{B}$ and velocity fields $\boldsymbol{V}$ along with the incompressibility condition $\beta \gg 1$.

The proportionality factor turns out to be

$$\alpha_\pm = \left[-\frac{k}{2} \pm \left(\frac{k^2}{4} + 1 \right)^{1/2} \right], \tag{10}$$

yielding the nonlinear dispersion relation

$$\omega = \alpha k_s, \tag{11}$$

where k_s is the projection of the wave vector along the ambient field $\boldsymbol{B}_0 = B_0 \widehat{e}_s$.

As stated earlier, in the limit $k \ll 1$, the MHD Alfvénic state

$$\alpha \to \pm 1, \omega \to \mp k_s, \tag{12}$$

with k independent relationships for both the co- and the counter propagating waves, is dutifully recovered.

For $k \gg 1$, it is easy to recognize, in analogy with the linear theory, that the (+) wave is the shear-cyclotron branch, while the (−) represents the magneto-sonic-whistler mode. The frequency of the (+) wave approaches some fraction of the ion gyro frequency (normalizing frequency) – it is only when $\boldsymbol{k}$ and $\boldsymbol{B}_0$ are fully aligned ($\widehat{k} \cdot \widehat{e}_s = \pm 1$) that the wave reaches the cyclotron frequency asymptotically. The fluctuation relation given by Eq. (9) will provide a crucial element in the construction of the kinetic and magnetic energy spectra.

The HMHD equations (7-8) may be manipulated to extract the well-known invariants [3],

$$\text{Total Energy} \quad E = \frac{1}{2}\int (V^2 + B^2) d^3x = \frac{1}{2}\sum_k |V_k|^2 + |B_k|^2, \tag{13}$$

$$\text{Magnetic Helicity} \quad H_M = \frac{1}{2}\int \boldsymbol{A} \cdot \boldsymbol{B} d^3x = \frac{1}{2}\sum_k \frac{i}{k^2}(\boldsymbol{k} \times \boldsymbol{B}_k) \cdot \boldsymbol{B}_{-k}, \tag{14}$$

$$\text{Generalized Helicity } H_G = \frac{1}{2}\int (\boldsymbol{A}+\boldsymbol{V})\cdot(\boldsymbol{B}+\nabla\times\boldsymbol{V})d^3x$$
$$= \frac{1}{2}\sum_k \left[\frac{i\boldsymbol{k}\times\boldsymbol{B}_k}{k^2}+\boldsymbol{V}_k\right]\cdot[\boldsymbol{B}_{-k}-i\boldsymbol{k}\times\boldsymbol{V}_{-k}], \quad (15)$$

where $\boldsymbol{A}$ is the vector potential. Notice that H_G & H_M are combinations of the kinetic and the cross helicities.

Since the relationship between $\boldsymbol{V}_k$ and $\boldsymbol{B}_k$ in HMHD were just now shown to be k dependent, it is expected that the current spectral predictions will be substantially different from those of the standard MHD (where $\boldsymbol{V}_k$ and $\boldsymbol{B}_k$ have identical spectra) particularly in the range $k \gg 1$ when the Hall term in Eq. (6) dominates. The introduction of the Hall term, which brings in an intrinsic scale (the ion skin-depth) removes the MHD spectral degeneracy and generates new scale-specific effects.

4. Spectral energy distributions

In order to derive the spectral energy distributions we resort to the Kolmogorov hypothesis according to which the spectral cascades proceed at a constant rate governed by the eddy turn over time $(kV_k)^{-1}$. For ε_E denoting the constant cascading rate of the total energy E, Eq.(13) along with Eq. (9) yields the dimensional equality

$$(kV_k)[1+(\alpha)^2]\frac{V_k^2}{2} = \varepsilon_E. \quad (16)$$

The omnidirectional spectral distribution function $W_E(k)$ (kinetic energy per gram per unit wave vector V_k^2/k), then, takes the form

$$W_E(k) = (2\varepsilon_E)^{2/3}\,[1+(\alpha)^2]^{-2/3}k^{-5/3}. \quad (17)$$

Consequently Eq. (9) yields:

$$M_E(k) = (\alpha)^2 W_E(k). \quad (18)$$

where $M_E(k) = B_k^2/k$ is the similarly defined omnidirectional spectral distribution function of the magnetic energy density.

The cascading of the magnetic helicity H_M (ε_H being the cascading rate for helicity) produces a different dimensional equality

$$(kV_k)\left(0.5\frac{B_k^2}{k}\right) = \varepsilon_H, \quad (19)$$

resulting in the following different kinetic and magnetic spectral energy distributions:

$$W_H(k) = (2\varepsilon_H)^{2/3}\ (\alpha)^{-4/3}k^{-1}, \quad (20)$$

$$M_H(k) = (\alpha)^2 W_H(k). \quad (21)$$

Finally, the cascading of the generalized helicity with a constant rate ε_G gives

$$(kV_k)\,[0.5g(k)V_k^2] = \varepsilon_G, \quad (22)$$
$$g(k) = (\alpha+k)^2k^{-1},$$

leading to the spectral energy distributions :

$$W_G(k) = (2\varepsilon_G)^{2/3}[g(k)]^{-2/3}k^{-5/3}, \tag{23}$$

and

$$M_G(k) = (\alpha)^2 W_G(k).$$

The energy spectra derived from the three invariants can be pieced together by using the experience gained from 2-D turbulence [4, 5]. It essentially boils down to placing the spectrum with the highest negative exponent of k at the highest k-end, and the one with the lowest negative exponent of k at the lowest k-end. The differential dissipation of the different invariants is the diktat behind this recipe. The poly-pronged kinetic and magnetic energy spectra can then be constructed.

5. Modeling solar wind spectra

Solar wind is a continuous, radial, supersonic outflow of plasma from the solar atmosphere and extends to the farthest reaches of the solar system to merge eventually with the interstellar medium at the earths orbit, electron- proton plasma with some trace elements has a density of 5-10 particles/cc, temperature $\sim$ 100,000 K and velocity $V \sim 300$ km/s. With small deviations from radial flow $\sim$ 10 km/s, it is collisionless, inhomogeneous and turbulent on several time and spatial timescales. The source of energy is the million degree solar corona; solar gravity is inadequate to hold the corona in static equilibrium. Chapman [6] suggested that geomagnetic storms are caused by plasma ejected at $\sim$ 1000 km/s from the solar flare. Biermann [7] proposed that sun is continuously emitting particles causing ionization and pointing away of cometary tails. First theory by Chapman, considered an extended corona with energy transfer only by conduction.

Hydrostatic equilibrium, however is no good! The electron density is too large to merge smoothly with the interstellar medium. Parker [8] suggested that the corona could not remain in static equilibrium but must be continually expanding since the interstellar pressure cannot contain a static corona. The continual expansion is called the solar wind. This was also known from comet observations but the properties predicted by Parker were confirmed by the satellites Lunik III and Venus I in 1959 and by Mariner II in the early 1960s. The main assumptions of Parker's model are that the outflow is steady, spherically symmetric and isothermal.

Due to solar rotation, the magnetic field lines are drawn into Archimedian spirals. Average field at the earth is 5 nanotesla with spiral angle of 45° with the radial. The direction either towards or away from the sun remains constant for several days. Transition is very abrupt. So inward and outward sectors are separated with a thin transition region. Fluctuations exist on three major scales: 11 year solar cycle related variations and fast stream slow stream interactions due to solar rotation; transient disturbances originating on the sun and propagating out; e.g. Solar flare caused blast wave with energy $\sim 10^{32}$ erg. On hours or less scales are the waves and turbulence in the plasma; e.g. Alfvén waves fluctuations have power law spectra k^{-p}, $p \sim 5/3$ along with other values. Key Observations of the solar wind turbulence:

1. velocity, density, magnetic field, and temperatures vary in time;
2. MHD accounted for fluctuations reasonably well, particularly Shear Alfvén waves, believing that the magnetosonic waves are damped by kinetic effects;
3. Alfvén waves are found always propagating outwards from the Sun;
4. similarity between power spectra of the magnetic fluctuations and the spectrum of velocity fluctuations for an isotropic magnetofluid as well as fluid turbulence;

5. turbulence driven by Stream- Shear Instabilities despite difficulties due to exact solutions, absence of evolution of Alfvén waves etc. It is not all Alfvén;

6. Voyager and Helios provided observations from 0.3 to > 30 AU;

7. reduced spectra are obtained by averaging over the two directions perpendicular to the solar wind velocity (V); spectra are a function of the wavenumber along V.

The spectral energy distributions of the velocity and the magnetic field fluctuations in the solar wind are now known in a wide frequency range– starting from much below the proton cyclotron frequency (0.1 - 1 Hz) to hundreds of Hz. The inferred power spectrum of magnetic fluctuations consists of multiple segments- a Kolmogorov like branch ($\propto f^{-5/3}$) flanked, on the low frequency end, by a flatter branch ($\propto f^{-1}$) and, on the high frequency end, by a much steeper branch ($\propto f^{-\alpha_1}, \alpha_1 \simeq$ 3-4), [9-14]. Attributing the Kolmogorov branch ($\propto f^{-5/3}$) to the standard inertial range cascade, initial explanations invoked dissipation processes (in particular, the collisionless damping of Alfvén and magnetosonic waves [14], to explain the steeper branch ($\propto f^{-\alpha_1}$, $\alpha_1 \simeq$ 3-4). However, a recent critical study has concluded that damping of the linear Alfvén waves via the proton cyclotron resonance and of the magnetosonic waves by the Landau resonance, being strongly k (wave vector) dependent, is quite incapable of producing a power-law spectral distribution of magnetic fluctuations [15]; damping mechanisms lead, instead, to a sharp cutoff in the power spectrum. Cranmer and Ballogoeijen [16] have however, demonstrated a weaker than an exponential dependence of damping on the wave vector by including kinetic effects. However, it is still steeper than that required for explaining the steepened spectrum.

An alternative possibility, suggested by Ghosh et al. [17], links the spectral break and subsequent steepening to a "change" in the "controlling" invariants of the system in the appropriate frequency range. Matthaeus et al. [18] have investigated the anisotropies in the spectral as well as in the variances of the 3-dimensional MHD turbulence. Stawicki et al. [19] have invoked the short wavelength dispersive properties of the magnetosonic/whistler waves to account for the steepened spectrum and christened it as the spectrum in the dispersion range. In this paper we follow and develop these ideas within the frame work of Hall-MHD. We will harness the three well-known invariants of HMHD [20,21]. Using dimensional arguments of the Kolmogorov type, we will first derive the fluctuation spectra associated with the velocity and magnetic fields. We then go on to show that in different spectral ranges, different invariants control the energy cascade splitting the inertial range into distinct sections. The steeper and the flatter spectral branches (together with the standard branch), then, are all sub-parts of the extended inertial range. Invoking the hypothesis of selective dissipation, we then construct the entire magnetic spectrum with its three branches and two breaks by stringing together three spectral segments each controlled by one of the three invariants. The observed frequency spectra of the solar wind are transformed into the wave vector spectra Doppler shifted by the Super Alfvénic Solar wind flow. Although the anisotropy of the MHD turbulence is now being highly emphasized [18], we model the observed reduced omnidirectional spectra with the findings of the isotropic cascade considered in section 4. The primary aim is to highlight the crucial contributions of the Hall effect. This, we believe, is being done for the first time. We will, in addition, indicate briefly how anisotropy issue can be addressed within the framework of Hall-MHD. Our intention is to show that the three spectral distributions derived in Sec. 4. can model the three branch spectrum ($k^{-1}, k^{-5/3}, k^{-\alpha_1} \alpha_1 \simeq 3-4$) of the magnetic fluctuations in the solar wind.

If the turbulence is dominated by velocity field fluctuations ($V_k^2 \gg B_k^2$) (which happens, according to Eq. (9), for ($\alpha \ll 1$), or ($k \gg 1$) for $\alpha \simeq (k^{-1})$, the spectral expressions under the joint dominance of the Hall term and the velocity fluctuations ($k \gg 1$) simplify to

$$W_{E_1}(k) = (2\varepsilon_E)^{2/3} k^{-5/3}, \quad M_{E_1}(k) = (2\varepsilon_E)^{2/3} k^{-11/3}. \tag{24}$$

$$W_{H_1}(k) = (2\varepsilon_H)^{2/3}k^{1/3}, \quad M_{H_1}(k) = (2\varepsilon_H)^{2/3}k^{-5/3}, \tag{25}$$

$$W_{G_1}(k) = (2\varepsilon_G)^{2/3}k^{-7/3}, \quad M_{G_1}(k) = (2\varepsilon_G)^{2/3}k^{-13/3}. \tag{26}$$

In the case wherein $\alpha = 1$ for $k \ll 1$, one obtains the standard Alfvénic state with $V_k \propto B_k$, and the corresponding spectra are (suffix 1 is used for the Hall Dominant and 2 for the standard MHD limit):

$$M(k) = W(k), \tag{27}$$

$$W_{E_2}(k) = (2\varepsilon_E)^{2/3}k^{-5/3}, \tag{28}$$

$$W_{H_2}(k) = (2\varepsilon_H)^{2/3}k^{-1}, \tag{29}$$

$$W_{G_2}(k) = (2\varepsilon_G)^{2/3}k^{-1}. \tag{30}$$

For the second root of $\alpha \simeq k$, $k \gg 1$, representing the whistler type fluctuations, we find the following spectra:

$$W_{E_w}(k) = (2\varepsilon_E)^{2/3}k^{-3}, \quad M_{E_w}(k) = (2\varepsilon_E)^{2/3}k^{-1}, \tag{31}$$

$$W_{H_w}(k) = (2\varepsilon_H)^{2/3}k^{-7/3}, \quad M_{H_w}(k) = (2\varepsilon_H)^{2/3}k^{-1/3}, \tag{32}$$

$$W_{G_w}(k) = (2\varepsilon_G)^{2/3}k^{-7/3}, \quad M_{G_w}(k) = (2\varepsilon_G)^{2/3}k^{-1/3}. \tag{33}$$

The observed solar wind magnetic spectrum will be generated if we were to string together the three branches $M_{E_1}(k)(\propto k^{-11/3})$, $M_{H_1}(k)(\propto k^{-5/3})$, and $M_{H_2}(k)(\propto k^{-1})$. The rationale as well as the modality for stringing different branches originates in the hypothesis of selective dissipation. It was, first, invoked in the studies of two-dimensional hydrodynamic turbulence [5]. The idea is that in a given k range, the particular invariant which suffers the strongest dissipation, controls the spectral behavior (determined, in turn, by arguments a la Kolmogorov). Thus if the k ranges associated with different invariants are distinct and separate, we have a straightforward recipe for constructing the entire k-spectrum in the extended inertial range. In 2-D hydrodynamic turbulence, for instance, the enstrophy invariant, because of its stronger k dependence (and hence larger dissipation) compared to the energy invariant, dictates the large k spectral behavior. Therefore, the entire inertial range spectrum has two segments- the energy dominated low k, and the enstrophy dominated high $k(\propto k^{-3})$. The procedure amounts to placing the spectrum with the highest negative exponent at the highest k-end, and the one with the lowest negative exponent of k at the lowest k-end.

The magnetic spectrum $M(k)$ and the kinetic spectrum $W(k)$, constructed by following the procedure delineated above, are shown in Fig.(1a) for the shear Hall fluctuations (Eqs. 24-26), in Fig.(1b) for the whistler fluctuations. (Eqs. 31-33), for the Hall dominated regime and in Fig. (2) for the Alfvénic state (Eqs. 27-30).

Notice that the observed solar wind magnetic spectra consisting of the branches $k^{-\alpha_1}$ ($\alpha_1 \sim 3-4$), $k^{-5/3}$ and k^{-1} can be reproduced by stringing the Hall state spectral branches (Fig.(1a)) at large k with Alfvénic state branches (Fig.(2)) at small k. The result is displayed in Fig. (3). This is rather fortunate because in HMHD it is precisely for large k that the Hall term is dominant while for small k, the standard Alfvénic behavior prevails.

There are three breaks in the spectrum displayed in Fig.(3). The break at k_1 is due to the change in the nature of turbulence from Alfvénic (M_{H_2}) to the Hall dominated state (M_{H_1}). The other breaks are due to changes in the controlling invariant (in the Hall dominated regime): at k_2 the control is transferred from magnetic helicity H_M to the total energy E, and at k_3 from the total energy E to the generalized helicity H_G. The entire spectrum for $k > k_1$ is a consequence of Hall dominance.

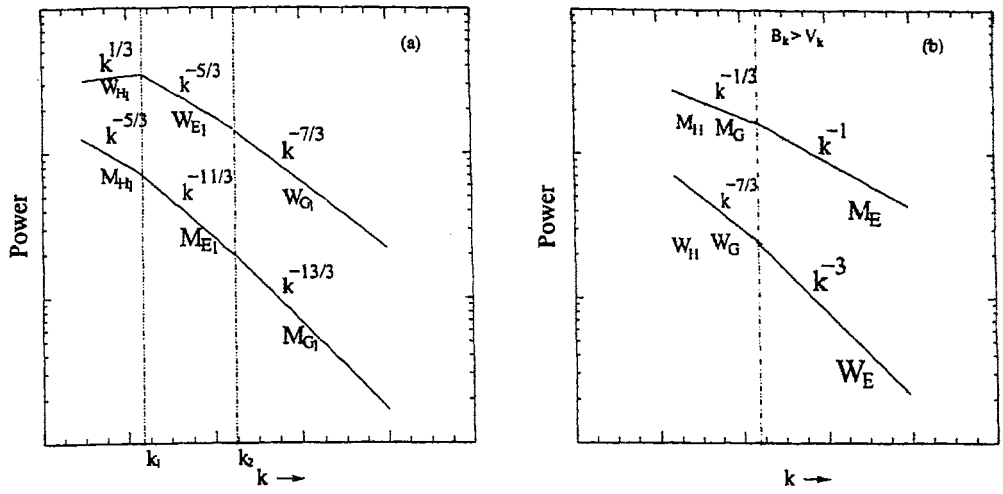

Figure 1: (a). Schematic magnetic energy (M) and Kinetic energy (W) spectra (Shear-cyclotron mode) for $\alpha = k^{-1}$ in the Hall region ($k \gg 2$), (b). Schematic magnetic energy (M) and Kinetic energy (W) spectra (Whistler mode) for $\alpha = k$ in Hall region ($k \gg 2$).

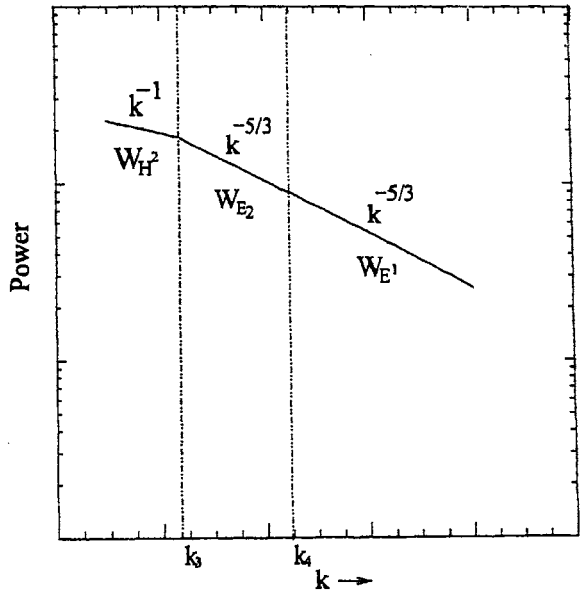

Figure 2: Schematic magnetic energy (M) and Kinetic energy ($W \equiv M$) spectra (shear-Alfvén mode) for $\alpha \simeq 1$ in the Alfvén region ($k \ll 1$).

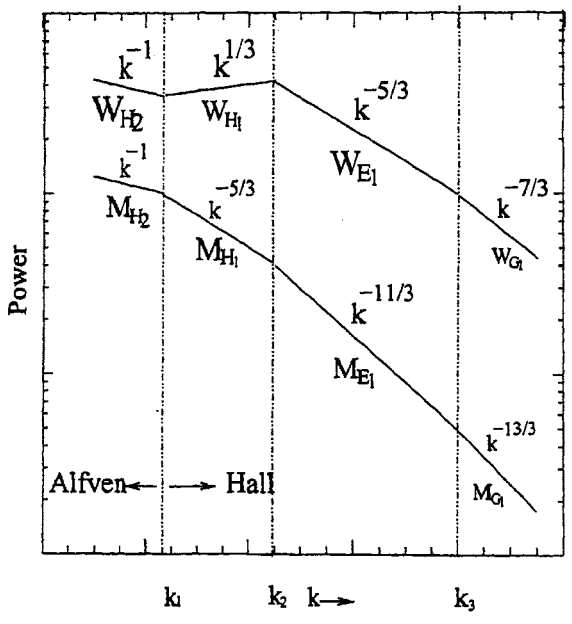

Figure 3: Modeled magnetic energy (M_1) spectra along with the corresponding Kinetic (W_1) spectra.

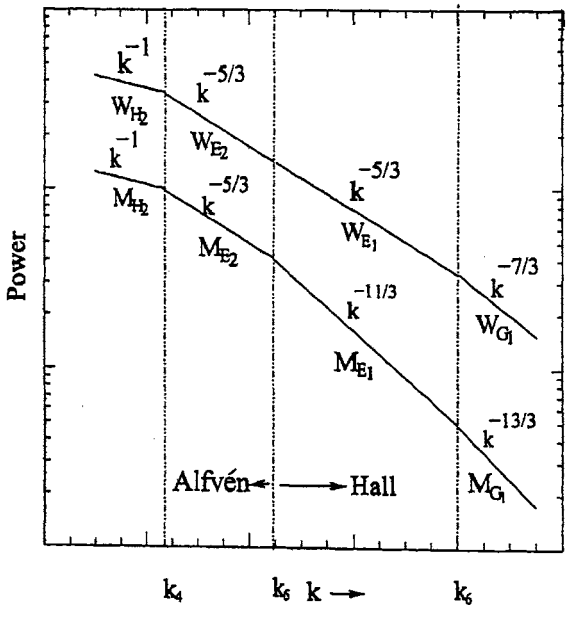

Figure 4: Modeled magnetic energy (M_2) spectra along with the corresponding Kinetic (W_2) spectra.

We must reiterate that the steepened branches $\propto k^{-11/3}$ and $k^{-13/3}$ are, here, very much a part of the inertial range; they have no connection to the dissipative range invoked in previous studies. The break at k_2 may lie near the observed break near $f \simeq 1$Hz.

Within the framework of this dimensional Kolmogorov- inspired model, there is another consistent way of constructing the observed magnetic spectrum of the solar wind from the spectral relations we derived. Since the branch $k^{-5/3}$ is common to the Alfvénic and the Hall dominated cases one could just as well assume that the change from Alfvénic to the Hall dominated state takes place at k_5 (Fig.(4)) instead of at k_1 as was assumed for the spectrum of Fig.(3). Notice that due to this replacement, the kinetic energy spectrum of Fig.(4) is quite different from that of Fig.(3) in the relevant k range. In the literature, k_5 has been identified with the strong damping region of the Alfvén mode via the proton cyclotron resonance [12, 13,].

Thus we find that there are two pathways of reproducing the observed magnetic spectrum depending upon the location of the spectral breaks. In principle, a somewhat detailed knowledge of the system would allow one to choose the more likely pathway. One would need to find in what range of k the standard Alfvénic description yields to Hall dominance and to what break in the spectrum that k corresponds. The absolute values of the breaks will, naturally, depend upon the numerical values of the parameters of the system.

Within the frame work of the Kolmogorov hypothesis combined with the selective dissipation hypothesis, the positions of the spectral breaks (k_2, k_3, k_4, k_6) indicate the scales of energy injection. The energy injected at k_2, e.g., will cascade towards large k as $k^{-11/3}$ and towards small k as $k^{-5/3}$. This is analogous to the 2-D turbulence where the energy cascades to small k as $k^{-5/3}$ and to large k as k^{-3}, a consequence of the two invariants, the energy and the enstrophy. This applies to other breaks at k_3, k_4 and k_6. The breaks at (k_1, k_5) , on the other hand, represent smooth transitions between the Hall dominanted and Alfvén states. The observed solar wind magnetic spectrum (M_1) ($k^{-11/3}$, $k^{-5/3}$, k^{-1}), in this context, has two scales of energy injection at (k_2, k_3) while k_1 signifies the change of guard from Alfvén ($k \ll 1$) to the Hall ($k \gg 1$) state; the latter is not a sharp break, instead the transition is smooth because M_{H_1} (Eq. 25) and M_{H_2} (Eq. (29)) are just limits of the smooth function $M_H(k)$ of Eq. (21). The break point k_2, determined from $M_{E_1}(k_2) = M_{H_1}(k_2)$, takes on the value $k_2 = (\varepsilon_E/\varepsilon_H)^{1/3}$) reflecting the dependence on the injection rates (also the dissipation rates) of the two invariants. Similar arguments apply to the spectrum M_2.

One would also do well to note that the branch $k^{-5/3}$ exists both in the Alfvén as well as the Hall state but in the former it is associated with the invariance of the total energy E and in the latter, with that of the magnetic helicity H_M. The k^{-1} branch, however exists only in the Alfvén state. As expected the entire spectrum is dominated by the Hall effect at large k and the Alfvén effect at small k and the energy injection scales lie at the high k end of the spectrum. This is symptomatic of the inverse or the dual cascade processes. It is clear that the spectrum of whistler fluctuations (Fig.(1b)) cannot account for the observed solar wind magnetic fluctuations. The reason for the unobservability of this spectrum may lie in the stronger damping of the whistler waves. It is also a well documented fact that out of the two possible types of turbulent fluctuations viz Alfvénic and magnetosonic, it is the former that is more likely to be observed [22]. The shear Alfvénic fluctuations suffer strong damping only when their frequency approaches the ion cyclotron frequency and this happens in HMHD only when k is strictly along the ambient magnetic field. Thus in general, the Alfvénic fluctuations suffer less damping than the magnetosonic/ whistler fluctuations. Although, we have, here, presented an isotropic view of the turbulent fluctuations, the polarization of the Alfvénic fluctuations, i.e. with amplitudes (V, B) perpendicular to the propagation vector k and the nonlinear nature of the cascade time (kV_k) immediately reflects the anisotropy of the turbulence. However, we defer the discussion of this issue until a more quantitative model based on the nonlinear interactions among the fluctuations is developed and this is underway. By including the physics of

the Hall current and the fluid vorticity in two-fluid magneto-hydrodynamics, the steepened part of the solar wind spectrum is shown to arise in the inertial range as contrasted with the dissipative range invoked in some earlier studies. The steepening in the present model is a consequence of the $(\boldsymbol{V}, \boldsymbol{B})$ relation enshrined in Eq. (9). This exact nonlinear relationship forbids any coupling between the right travelling waves with each other or the left travelling waves with each other. However the coupling between the left travelling and the right travelling waves remains and this is expected to provide a theoretical model of turbulence as in the standard Alfvénic turbulence [23]. There is another way of obtaining the (V, B) relation. This is done by invoking the variational principle and the selective decay hypothesis [3] leading to the double Beltrami conditions which reduce to the (V,B) relation given in Eq.(9) in the large k limit. We have also shown that this form of the relation is obeyed by the shear wave in the Hall regime. In a final summary, our Hall MHD model predicts: (i) an extended inertial range with $k^{-11/3}$ along with $k^{-13/3}$ at high k-end, and (ii) related but not identical spectra for the kinetic and the magnetic fluctuations. However, the issues of anisotropy and the detailed nature of cascades through mode interactions at a realistic value of β need to be addressed before the model can be taken to represent the reality of the solar wind. It is intriguing that Stawicki et al. [24] have attributed the steepening (limited to k^{-3}) to the higher dispersion of the Alfvén waves at large k_z, using the associated time scale and introducing the term 'Dispersion range'. In contrast the physics at large k in the framework of Hall-MHD (Hall currents become important even dominant at large k) contributes to steepening in a markedly different way; the new non-Alfvénic relationship between $\boldsymbol{V}$ and $\boldsymbol{B}$ predicting steepening is a consequence of the shear Hall mode. It is this high k behavior that dictates related but different spectra for the magnetic and kinetic fluctuations as distinguished from Stawicki et al. [24] where the two spectra are identical. Thus there are at present different ways and approaches of modeling the solar wind spectrum and further investigations would provide the clues to the real nature of the solar wind turbulence.

6. Modeling of solar atmospheric turbulence

We shall now test the spectral predictions of HMHD against the observations on the velocity and the magnetic fields on the solar surface. The existence of velocity fields in the form of convective cellular patterns of different characteristic spatial dimensions has been known for a long time. This phenomenon known as the solar granulation has been quantified in terms of the spectral energy distributions of kinetic energy with a Kolmogorov spectrum $k^{-5/3}$ at small spatial scales which flattens to a $\sim k^{-0.7}$ form towards larger spatial scales [25, 26]. The hierarchical distribution of velocity and magnetic fields on the solar atmosphere with the inferred spectral exponents of the non Kolmogorov type (e.g. (1.3), (-1), and (-0.7)) [25-28] cannot be accounted for by those existing in the literature [29-31] due to inadequate treatment of magnetic turbulence (in contrast to the inadequate treatment of hydrodynamics). This spectrum was modeled by invoking the inverse cascade of energy in a helically turbulent medium [27]. More recently, with the availability of the velocity information on supergranular scales, the predictions of the inverse cascade model have been further examined [32, 33]. However, these studies do not address the question of the corresponding distributions of the solar magnetic field. Now that the spectral distributions of the solar magnetic field are beginning to be inferred from magnetogram observations, it becomes necessary to determine the velocity and the magnetic field distributions in a coupled magneto-fluid medium. Recently Lee *et al.* [28] have reported the magnetic power spectra of the network and the non-network fields and displayed them along with the kinetic energy power spectrum (Fig. 5) in a much wider range of scales and with better procedures to take care of the seeing and noise embellishments than the previous attempts [30,34]. We find that the spectra M_{E_1} (Eq.24) and M_{H_2} (Eq. 29) account very well for the observed spectra (Fig. 5) in the range $0.5\ Mm^{-1} < L < 10 Mm^{-1}$. We must emphasize that the concurrent

existence of $k^{-5/3}$ spectrum for the kinetic energy and $k^{-11/3}$ for the magnetic energy density is a result of the inclusion of the Hall term which allows a relationship of the type given in Eq. (9). Restricting various branches to their respective regions of validity defined by the diktats of the differential dissipation, our construction for the kinetic and magnetic energy spectra in the full k range is displayed in Fig. 6.

The flat part of the observed network field spectrum and the positive exponent part (1.3) of the non-network field spectrum still remain to be modeled. For $\alpha \approx k$ and thus $\boldsymbol{B}_k = k\boldsymbol{V}_k$ for the whistler type fluctuations we find the magnetic spectrum from the magnetic helicity cascade as well as from the cascade of the total energy to be:

$$M_H \propto k, \tag{34}$$

for the choice of the inverse of the cascade time $k(V_k/V_A)^{n/m+n}$, where n tends to 1 and $(m+n)$ tends to 0.

This shows that in this region $\boldsymbol{V}_k \approx \boldsymbol{V}_A$. The corresponding kinetic spectrum is

$$W_H \propto k^{-2} M_H. \tag{35}$$

The observed exponent (1.3) for the magnetic spectra M_H and the corresponding kinetic energy spectrum is $W_H \propto k^{-0.7}$ could be approximately taken to agree with the theoretically derived exponents (1) and (-1) respectively. We must recall that at large k where $\alpha \approx k^{-1}$ applies, the relation between the kinetic and the magnetic spectral energies is $W_E \propto k^2 M_E$ in contrast to the relation at small k where $W_E \propto k^{-2} M_E$. Now the flat part ($\sim\propto k^0$) of the network field obtains for $(m/n) = -1/2$ corresponding to the cascade time scale ${V_k}^2/V_A$; it can also used by invoking the interaction between Alfvén wavepackets. The kinetic energy spectrum $W_H \propto k^{-2}$. The entire spectrum with its various branches are exhibited in Fig.(6). The impressive reproduction of the observed spectra from this theoretical model comes with a prediction - the kinetic energy spectral branch corresponding to the flat part of the non network magnetic field goes as ($\propto k^{-2}$). This range is yet to be observationally investigated. There are additional issues such as the nature of the spectra when the magnetic field may be dominant and the presence of anisotropy if any. These can be addressed as and when the need and the motivation provided by the observations become compelling.

Is it merely fortuitous that the incompressible Hall MHD appears to reproduce the observed solar spectra? How is it that the collisional solar photospheric plasma honours the invariance of the energy and the kinetic and the magnetic helicities and their attendant consequences? We do not claim a deep enough comprehension of this system to really answer these questions but plausibility arguements could, perhaps, be advanced. The Kolmogorov law of (-5/3) seems to hold for gravitationally stratified astrophysical plasmas in a variety of situations including the solar atmosphere. One reason is that the velocity fields are small compared to the sound speed and the motions are essentially incompressive. In a magnetized plasma this condition can be described in terms of plasma beta being greater than unity as it is on the solar surface. In other words the plasma is stratified/compressive but the turbulence that determines the spectrum, is incompressive. We must also point out that the solar photospheric plasma is partially ionized with electron density = 10^-4 of the neutral density at the photosphere and this fraction increases as the temperature increases towards the chromosphere. It is found that the electron-ion collision frequency is smaller than the electron- neutral collision frequency which is larger than the ion - neutral collision frequency by the factor $(m_i T_e/m_e T_i)^{0.5}$ [36, 37]. This implies that the photospheric plasma is indeed a three fluid plasma and electrons and ions form two distinct fluids and hence the Hall MHD.

The Hall scale $L_H = \lambda_i/M_A$ at which the inductive term $(\boldsymbol{V} \times \boldsymbol{B})/c$ becomes equal to the Hall current term $(\boldsymbol{J} \times \boldsymbol{B}/nec)$ in the generalized Ohm's law turns out to be $\simeq 0.5$km for the solar

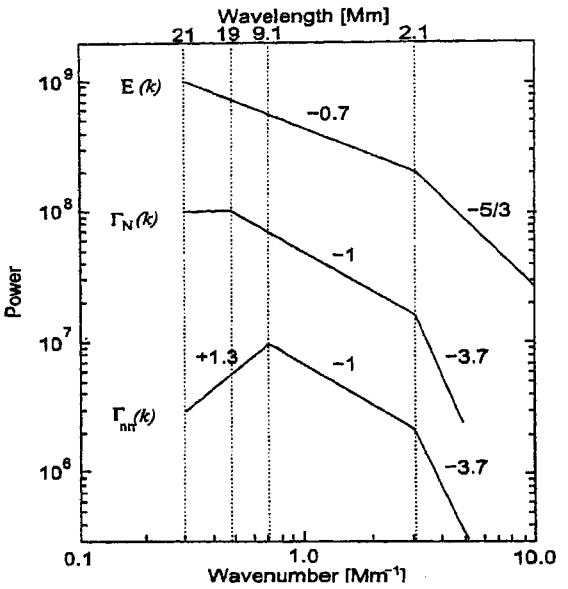

Figure 5: Schematic spectral regimes of the network field spectrum ($\Gamma_N(k)$) and those of the non-network field spectrum ($\Gamma_{n-N}(k)$) found in the present study. These are compared with the schematic Power spectrum of Dopplerogram $E(k)$; [25a],[28].

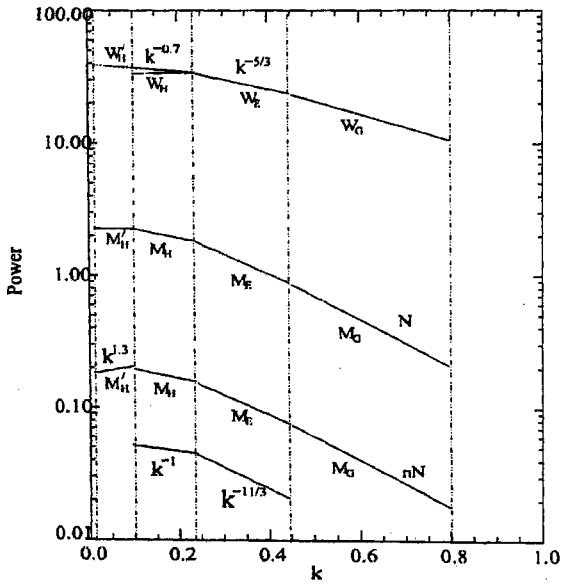

Figure 6: Power spectra of kinetic energy (W) and magnetic energy (M) for network (N) and non-network (nN) fields.

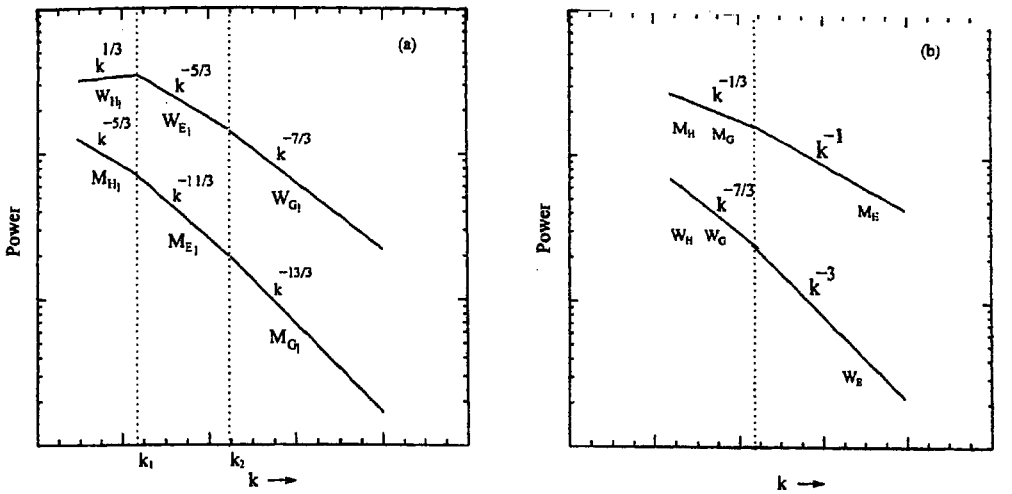

Figure 7: a) Schematic magnetic energy (M) and Kinetic energy (W) spectra in the Hall state for $\alpha_+ \to 1/k$, ($k \gg 1$). b) Schematic magnetic (M) and Kinetic (W) spectra in the Hall state for $\alpha_- \to -k$, ($k \gg 1$).

photosphere [36, 38] where $M_A \simeq 4 \times 10^{-3}$ is the Alfvén Mach number and the ion skin depth $\lambda_i \simeq 2.4$cm for photospheric electron density $n \simeq 10^{14}\text{cm}^{-3}$.

The Hall scale L_H is much smaller than any observed velocity and magnetic scale ($\geq$ 1000km). However, in the double beltrami states, the scales of the field variations are determined by a joint action of the ion skin length and the constants a and b- which in turn, are to be evaluated from the values of the constants of motion. For a system in which the velocity field is relatively large, one of the effective scale lengths can be several orders of magnitude larger than λ_i . The point is that the Hall term (coupled with the fluid vorticity term) introduces a singular perturbation in the standard MHD and even though it may have a small coefficient multiplying it, it can and does have a profound effect on the system dynamics.

The Hall dynamics as distinct from the Alfvénic dynamics allows states in which the kinetic energy and the magnetic energy are not equipartitioned. Our experience with solar spectra fitting appears to support the absence of equipartition in the range of spatial scales considered here. It would be instructive to examine this feature on larger spatial scales such as those of supergranulation and the giant cells. There are additional issues of the existence of a large scale magnetic field and the ensuing anisotropy as well as the physical model of the Hall-MHD turbulence in terms of the Hall-Alfvén and other waves along with the confirmation of the Kolmogorovic results by direct numerical simulations which must be addressed in order to take this study to its logical conclusion.

7. Laboratory experiments

Recently, the universality of the large scale turbulence with the kinetic energy spectrum going as $k^{1/3}$ has been concluded from the laboratory experiments on MHD turbulence [39]. Evidence in favor of such a spectrum has also been seen in convective atmospheric boundary layer [40, 41] along with the usual Kolmogorov spectrum $k^{-5/3}$. The Cirrus clouds [42] have too been observed to support $k^{1/3}$

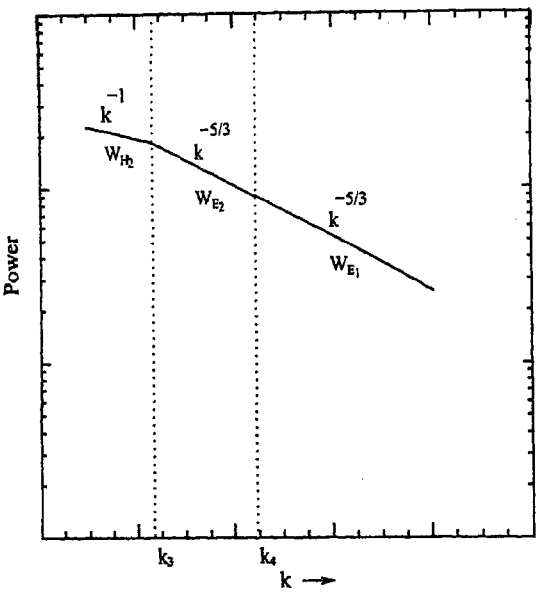

Figure 8: Schematic magnetic energy (M) and Kinetic energy ($W \equiv M$) spectra in the Alfvén state ($k \ll 1$).

spectrum. While some of the spectral predictions of the Hall-MHD found ratification in the solar turbulence, the 1/3 kinetic energy spectrum could not be tested due to lack of observations on those scales. Although the 1/3 spectrum has been theoretically derived invoking the conservation of the total energy flux [39] in a given volume, we show that the Hall-MHD with its new features offers a better alternative. We observe that the spectral branch $k^{1/3}$ of the kinetic energy spectrum originates from the magnetic helicity invariant H_M under the dominance of the Hall effect ($k >> 1$) as well as that of the kinetic energy ($V_k >> B_k$) for $\alpha_+ \to 1/k$, and it should operate in large spatial scale regime as dictated by the hypothesis of selective dissipation. In the Alfvén regime($k \ll 1$) the corresponding spectral branch $W_{H_2}(k) \propto (k^{-1})$. There are two breaks in the spectra displayed in Figs.(7a,7b) and one break in Fig. (8). They are due to the change of the controlling invariant: at k_1, the control is transferred from magnetic helicityH_M to the total energy E and at k_2, from the total energy E to the generalized helicity H_G. Within the framework of the Kolmogorov Hypothesis combined with the selective dissipation hypothesis, the positions of the spectral breaks indicate the scales of energy injection. The energy injected at k_2, e.g., will cascade towards small k as $k^{-5/3}$ and towards large k as $k^{-7/3}$. Similarly the energy injected at k_1 will cascade towards large k as $k^{-5/3}$ and towards small k as $k^{1/3}$. This is also in agreement with the conclusions of the papers 1 and 2. The $k^{1/3}$ spectrum in given in [35] is derived by invoking the constancy of the total energy flux in the entire volume (k^{-3}) i.e. dimensionally $(kV_k)(V_k{}^2)(k^{-3})$= constant. In contrast our derivation relies on the global invariant H_M. Although the two approaches are dimensionally identical, the underlying physics is very different. Additionally our small spatial scale spectra also show the steepened $k^{-7/3}$ branch comparable to the spectral branches A, B and C of [1]. We propose that the measurement of the concomitant magnetic energy spectrum which should carry much less energy than the kinetic spectrum ($V_k \gg B_k$) may shed light on the type of the controlling invariant.

8. Conclusion

The distinguishing features of the Hall-turbulence model, and the main ingredients of calculations are:

1. use of Hall instead of ideal MHD,
2. exploitation of the generalized helicity as an invariant in addition to the total energy and the magnetic helicity,
3. the surmise that the relations (Eqs. (9)) between $\boldsymbol{V}$ and $\boldsymbol{B}$ provided by the nonlinear solutions of the Hall-MHD equations operate at large or small k depending upon the predominance or otherwise of the velocity field *vis a vis* the magnetic field,
4. Kolmogorovic dimensional arguments are used to derive various spectra from the cascading of the invariants,
5. differential dissipation of the invariants is invoked in order to fix the relative positions of various spectral branches,
6. the solar spectra are modeled by invoking the fact that on the solar surface the hydrodynamic motions are dominant (much greater energy in kinetic energy fluctuations as compared to the magnetic fluctuations) so that $\alpha \approx k^{-}1(k)$ apply at large (small) k,
7. the cascade time scale is a combination of the hydrodynamic and the Alfvén timescales.
8. the difference between the network and non-network magnetic field spectra may be due to the relative contributions of the hydrodynamic and the Alfvén time scales.

In fact since the velocity and magnetic fluctuations are related through α, there are no purely hydrodynamic or magnetic timescales. The laboratory detection of the kinetic spectra with 1/3 exponent is amply accounted for by the Hall turbulence model. The dimensional basis of this model need to be given a sound theoretical base in the near future.

Acknowledgments: The authors thank Dr. Baba Varghese for his help in the preparation of this manuscript.

References

1 Walén C, *Ark. f. mat. astr. o. fys*, 30A (1944), no. 15 and 31B, no. 3;
Alfvén H, Falthämmer C, *Cosmical Electrodynamics* (Clarendon Press, Oxford, 1963);
Parker P N, *Cosmic magnetic fields*(Clarendon Press, Oxford, 1979).
2 Mahajan S M, Krishan V , *Phys. Rev. Lett.* (2004), submitted.
3 Yoshida Z, Mahajan S M, *Phys. Rev. Lett.*, (2002), 88.
4 Fjortoft R, *Tellus*, 5 (1953), 525.
5 Hasegawa A, *Advances in Phys.*, 34(1985), 1.
6 Chapman S, *Proc. Roy. Soc.*, A95(1929), 61.
7 Biermann L, *Z. Astrophys.*, 29(1951), 274.
8 Parker E N, *Astrophys. J.*, 128(1958), 664.
9 Coleman P J Jr., *Astrophys. J.*, 153(1968), 371.

10 Behannon K W, *Rev. Geophys. & Space Phys.*, 16 (1978), 125.
11 Denskat K U, Beinroth H J, Neubauer F M, *J. Geophys.*, 54(1983), 60.
12 Gary S P, *Theory of Space Plasma Microinstabilities*, Cambridge Univ. Press, New York, (1993).
13 Leamon R J, Smith C W, Ness N F, Matthaeus W H, Wong H K, *J. Geophys. Res.*, 103 (1998), 4775.
14 Gary S P, *J. Geophys. Res.*, 104(1999), 6759.
15 Li H, Gary P, Stawicki O, *Geophys. Res. Lett.*, 28(2001), 1347.
16 Cranmer S R, von Ballagooijen A A, *Astrophys. J.*, 594(2003) 573.
17 Ghosh S, Siregar E, Roberts D A, Goldstein M L, *J. Geophys. Res.*, 101(1996), 2493.
18 Matthaeus W H, Ghosh S, Oughton S, Roberts D A, *J. Geophys. Res.*, 101(1996), 7619.
19 Stawicki O, Gary P S, Li H, *J. Geophys. Res.*, 106(2001), 8273.
20 Mahajan S M, Yoshida Z, *Phys. Rev. Lett.*, 81(1998), 4863.
21 Krishan V, Mahajan S M, *Solar Physics.*, 220 (2004) 29.
22 Goldstein M L , Roberts D A, Matthaeus W H, *Ann. Rev. Astron. Astrophys.*, 33(1995) 283.
23 Shebalin J V, Matthaeus W H, Montgomery D, *J. Plasma Phys.*, 29(1983), 525.
24 Stawicki O, Gary P S, Li H, *J. Geophys. Res.*, 106(2001), 8273.
25 Muller R, *Solar and Stellar Granulation*, eds. R J Rutten, G Severino, Kluwer academic Publisher, Dordrecht, Holand,(1989), 101.
26 Zahn J A, *Solar and Stellar Physics Lecture Notes in Physics*, 292(1987) 55, eds. Schröter E W, Schüssler M, Springer Verlag, Berlin.
27 Krishan V, *Mon. Not. Roy. Astron. Soc.*, 250(1991), 50.
28 Lee Jeongwoo Chae J C , Yun H S, *Solar Phys.*, 171, (1997) 269.
29 Biskamp D, *Nonlinear Magnetohydrodynamics*, Cambridge University Press, Cambridge, (1993), 232.
30 Knobloch E, Rosner R, *Astrophys. J.*, 247(1981), 300.
31 Tennekes H, Lumley J L, *A First Course in Turbulence*, MIT Press, Cambridge, MA,(1972) Ch. 8.
32 Krishan V, Paniveni U, Singh Jagdev, Srikanth R, *Mon. Not. Roy. Astron. Soc.*, 334(2002), 230.
33 Paniveni U, Krishan V, Singh J, Srikanth R, 2003, *Mon. Not. Roy. Astron. Soc.*, (2003) (in press).
34 Nakagawa Y, Priest E R , *Astrophys. J.*, 179(1973), 949.
35 Branover H, Eidelman A, Golbraikh E, *Phys. Fluids*, 16(2004), 845.
36 Priest E R, *Solar Magnetohydrodynamics*, Reidel, Dordrecht, (1982), 83.
37 Chitre S M, Krishan V, *Mon. Not. Roy. Astron. Soc.*, 323 (2001), L23.
38 Priest E R, Forbes T, *Magnetic Reconnection*, Cambridge University Press, (2000), 44.
39 Branover H, Eidelman A, Golbraikh E, *Phys. Fluids* , 16 (2004), 845.
40 Kaimal J C, Eversole R A, Lenschow D H, Stankov B B, Kahn P H, Businger J A, *J. Atmos. Sci.* 39(1982), 1098.
41 Tjernstrom M, Friehe C A, *J. Atmos. Ocean. Tech nol.*, 8(1991), 19.
42 Gultepe I, Starr D O'C , *J. Atmos. Sci.* , 52(1995), 4159.